Electrical Power and Energy Systems 161 (2024) 110210

Contents lists available at ScienceDirect

International Journal of Electrical Power and Energy Systems

journal homepage: www.elsevier.com/locate/ijepes

A security-aware dynamic hosting capacity approach to enhance the integration of renewable generation in distribution networks

Leslie Herding [a,*], Leonel Carvalho [b], Rafael Cossent [a], Michel Rivier [a]

[a] Institute for Research in Technology (IIT), ICAI School of Engineering, Universidad Pontificia Comillas, C/Santa Cruz de Marcenado 26, 28015 Madrid, Spain
[b] INESC TEC, Rua Dr. Roberto Frias #378, 4200-465 Porto, Portugal

ARTICLE INFO

Keywords:
Flexible connections
Dynamic hosting capacity
Probabilistic analysis
N-1 contingencies
Distributed generation
Distribution grids

ABSTRACT

Hosting capacity (HC) describes the electricity network's ability to accommodate distributed generation (DG) without deteriorating electrical performance indicators. Distribution system operators typically express their networks' HC as a single threshold, called static hosting capacity (SHC). SHC is determined via conservative regulatory criteria, increasing connection costs and time. This paper explores the potential for additional energy injection into the network via dynamic hosting capacity (DHC). A network node's DHC is derived from the hourly operation of the network, accounting for the time variability of existing distributed generation (DG) output and demand. The methodology considers the network assets' N-1 contingencies and their probabilities, defining the security-aware DHC (SDHC). The SDHC definition is technologically neutral. Through a case study of a radial medium voltage distribution network, the paper highlights the significant limitations of SHC due to conservative calculation criteria mandated by regulators. Annual injectable energy is increased by 62% to 76% when comparing DHC to SHC. Variations between average DHC and SDHC are below 0.01% due to low N-1 probabilities. This finding points out the potential of dynamic hosting capacity definitions, allowing more efficient use of the existing network and facilitating the integration of new DG capacity with reduced connection costs and time.

1. Introduction

Significant additions of renewable energy sources (RES) into the distribution networks are expected over the following decades. The permitting process is one of the main bottlenecks for RES expansion, which is brought up frequently within the sector and is well-known by policymakers [1,2,3]. The electricity grid plays a significant role in integrating new RES generation [4]. Network congestion due to the increasing integration of distributed generation (DG) is already prevalent in European distribution networks [5]. The grid's capacity to integrate further generation or demand is denominated hosting capacity (HC). For the determination of a network node's available HC, the impact of connecting a new unit on performance indicators such as power quality is considered [6]. The capacity of RES that can be connected to the node without exceeding the limit of the performance index is the HC [7].

The European Commission encourages the publication of available network HC to provide transparency to RES promoters and direct connection requests to areas with available grid capacity [8]. Several distribution system operators (DSOs) already provide this information in the form of lookup tables or interactive maps [9,10,11,12,13]. These available HCs commonly represent a static threshold determined via regulatory criteria. However, due to the conservative criteria for calculating the network's HC, reinforcement requirements are often determined for assets that might only be used for a few hours per year [14]. This poses an unnecessary economic burden on connection seekers and increases connection times due to time-consuming network expansion works [8,15]. Flexibility mechanisms can be a valuable tool to reduce distribution network infrastructure investments [14]. One of those tools is flexible network access. Opposed to firm access, flexible network access allows for a more dynamic definition of the network capacity offered to a network user [8]. It represents the option for the DSO to define the network's HC more dynamically to adjust to the operational reality of demand and RES generation fluctuations instead of calculating a static hosting capacity (SHC) threshold as currently performed by most DSOs [5,16]. Increasing advances in digitalisation already performed or foreseen for the near future allow for more monitorisation and a more dynamic operation of electricity distribution grids

* Corresponding author.
E-mail address: lherding@comillas.edu (L. Herding).

https://doi.org/10.1016/j.ijepes.2024.110210
Received 29 February 2024; Received in revised form 2 July 2024; Accepted 27 August 2024
Available online 4 September 2024

[17]. A dynamic control of power injection according to the instantaneous performance of the grid may be expected, enhancing the viability of applying a dynamic HC approach.

Distribution grid HC for integrating RES has been subject to studies for years [6,7,18]. The literature can be categorised according to two dimensions: i) how HC is defined, and ii) the quantification methodology.

The definitions of HC uncertainty, stochastic HC, and locational HC have been reviewed in [19]. However, the HC of modern power systems is of a dynamic nature due to changing load patterns and variable RES availability. Stochastic HC contemplates uncertainties influencing the network's HC. Still, many stochastic HC evaluations define HC as a single threshold applied throughout the whole year [20]. A dynamic definition of HC can speed up the integration of RES into existing electricity networks [21]. A typical Scottish network's HC is evaluated for integrating wind energy via a deterministic and a dynamic probabilistic approach in [22]. The authors focus on determining the HC of the network as a whole rather than exploring the benefits of dynamic hosting capacity (DHC) over SHC. A weekly definition of DHC for integrating PV at a university building in Morocco is evaluated in [23]. The network node's DHC is calculated in the first step, and the optimal PV generator's size in the second step.

The HC of 17 real utility distribution feeders to integrate increasing penetrations of PV is evaluated via a genetic algorithm in [24]. HC is assessed via the Monte Carlo (MC) method based on maximum and minimum daytime load to express extreme operating scenarios. Final HC is determined via a conservative approach as the minimum of detected thresholds. A linear power flow algorithm for maximising a distribution network's HC is proposed in [6]. HC is considered a static threshold for different sets of nodes of the IEEE 33-bus network with no existing DG. A computationally efficient methodology to determine a network's SHC for integrating PV is proposed in [25]. The authors of [26] show via thermal models that implementing dynamic thermal transformer rating allows to connect PV capacity surpassing the rated transformer capacity. The benefits of a dynamic definition of HC for PV that allows for temporary violations of the network's operational limits are evaluated via quasi-static time-series analysis in [27]. In the dynamic evaluation, HC is 60 % to 200 % higher than SHC for the worst-case moment of maximum PV-to-load ratio. However, the final HC results obtained from the dynamic evaluation are presented as a static threshold of PV capacity.

Based on the limitations defined on the literature review, this work contributes the following:

1. **Evaluation of DHC over SHC:** Literature focuses on different HC definitions for integrating a specific technology, i.e. PV or wind power. This work employs an approach similar to the results presented in [23]. HC is evaluated from a network node's point of view, independent of a generation unit's size. The proposed methodology presents an approach to assess the benefits of dynamic hosting capacity versus static hosting capacity, with the latter being determined via conservative regulatory criteria currently applied in Spain, considered representative of common as-usual conservative criteria for SHC computations. DHC is subject to the operating conditions derived from RES and load which are represented as hourly curves to capture the variability throughout the year.
2. **Technologically neutral evaluation of HC:** Both SHC and DHC are calculated from a network perspective, i.e., technologically neutral, as DSOs require. This means that hosting capacity is presented as a network node's HC rather than the HC for a specific generation technology under evaluation. The modelling of DHC accounts for the uncertainty of renewable energy availability by employing several sample years in a combinatorial analysis and the time variability of the demand throughout the year. DHC and SHC are compared in terms of energy injection into the network.
3. **Definition of security-aware dynamic hosting capacity to account for network contingencies' probabilities impact on DHC:** The model includes an evaluation of the impact of contingency considerations for a holistic comparison with existing regulations. DHC is assessed one by one for all network assets' N-1 failures. The network nodes' security-aware dynamic hosting capacity is introduced. It is derived by determining the DHC for each N-1 contingency, accounting for the respective probability of occurrence of the N-1 contingency scenario. It is presented as an hourly annual curve instead of a single threshold, allowing RES promoters to plan their investment optimally.

The rest of the paper is organised as follows: the modelling methodology of SHC, DHC and SDHC is presented in 2, and the case study design, including model inputs, is presented in 3. Section 4 presents the results of the case study on the benefits of SDHC over SHC. Section 5 concludes the paper.

2. Methodology

This work assesses the benefits of a flexible definition of nodal HC that accounts for realistic operating conditions resulting from the variability of RES and load throughout the year. The results of the analysis are limited to the node under evaluation, similar to hosting capacities published by DSOs [9,10,11,12,13]. The following definitions of different HC concepts are employed throughout this paper:

- **Static hosting capacity (SHC)**: single HC threshold derived via conservative criteria of minimum load and maximum availability of existing generation.
- **Dynamic hosting capacity (DHC)**: hourly curve of HC accounting for operating results based on load and existing generation profiles.
- **Security-aware hosting capacity (SDHC)**: hourly curve of HC accounting for DHC under N-1 contingencies of all normally closed network elements and their probabilities of occurrence.

Fig. 1 summarises the methodology for obtaining HC in its different definitions. Network reconfigurations r are employed to account for N-1 contingencies of the network assets compared to normal operating conditions N, while hours h convert HC from a static threshold to a dynamic definition.

A network node's hosting capacity is determined as the maximum injectable active power. The nodal maximum injectable energy is obtained via optimal power-flow (OPF) analysis to ensure that operational security limits are not violated. Secure network operation is guaranteed via thermal line limits and maximum voltage deviations. Note that although voltage regulation mechanisms such as tap changers and inverter controls may provide additional value to implementing a DHC approach, they have been excluded from the study since not all distribution grid zones may be able to resort to these devices. Consequently, the results shown are conservative and focus on the impact of RES and load variability alone.

The OPF's objective function seeks the minimisation of system costs. Hence, ascending cost signals are employed to ensure the merit order within the network. This will not result in an economic dispatch of the system components but is used to ensure that the cost minimisation algorithm does not curtail preexisting generators or load to increase HC. Cost signals rank the merit order as follows:

1. **Existing generation capacity:** preexisting generators in the network must not be curtailed to inject more energy at the node under HC evaluation.
2. **HC evaluation node:** energy injected at the HC evaluation node.
3. **Import from the external grid:** electricity imports from the upstream network to cover local demand.

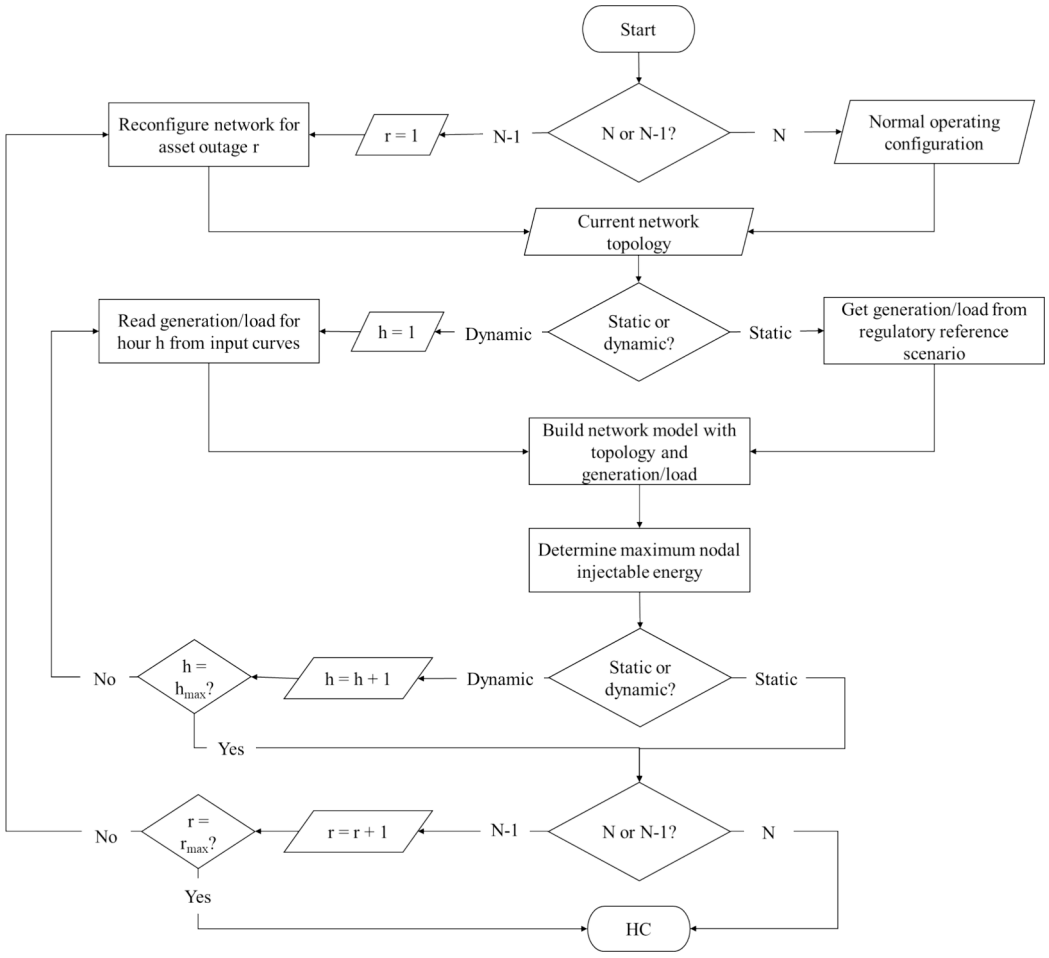

Fig. 1. Model flowchart for obtaining HC.

4. **Energy non-served:** load curtailments represent a last-resort mechanism to ensure the safe operation of the network within security limits.

Furthermore, some countries' regulations require the evaluation of HC accounting for short-circuit currents. For example, Spanish regulation defines the short-circuit ratio (SCR) for each distribution network node as [28] presented in Eq. (1), where Scc represents three-phase short-circuit power, and P_{MPEi} is the capacity of all N generation units connected at the node under analysis. SCR considerations are limited to the static evaluation under normal operating network configuration. Dynamic SCR due to different reconfigurations and varying demand/generation patterns are out of the scope of this work.

$$SCR = \frac{S_{cc}}{\sum_i^N P_{MPE_i}} \tag{1}$$

The result of the optimisation represents nodal HC. Different network nodes are evaluated in this study to obtain a broader understanding of SHC, DHC and SDHC. In this section, the criteria for the calculation of the different hosting capacities are described. SHC is calculated according to the regulatory requirements described in 2.1, and DHC modelling is described in 2.2. SDHC modelling is described in 2.3.

2.1. Static hosting capacity according to regulatory requirements

A node's SHC is the maximum injectable energy for the reference scenario without violating the operational security limits. Static hosting capacity is evaluated based on peak generation and valley load to guarantee the available HC at all hours. As for considerations of network unavailability, worst-case SHC is assessed under N-1 contingency conditions. SHC under N-1 contingencies is evaluated, including network reconfigurations to ensure service availability in case of asset failure. Dynamic network reconfiguration (DNR) is considered according to [29]. The multi-objective, multi-period DNR model aims to optimise the network topology by minimising the overall operation cost of a distribution system. The objective function considers the cost components outlined in [29]: i) Network power losses, and ii) Costs associated with lines and transformers overloading, and bus voltage violations. The DNR objective function is subject to four groups of constraints: power balance, power flow limits, switching operations, and topological constraints such as radiality. In this work, the employment of DNR is limited to the reconfiguration after asset failures and not as a HC enhancement technology to guarantee that the conclusions obtained result from the variability of RES and load.

SHC results are assessed for normal operating conditions (SHC N) and asset contingencies (SHC N-1).

2.2. Dynamic hosting capacity

Dynamic hosting capacity (DHC) is evaluated as the maximum hourly injectable energy without violating the operational security limits. The evaluated energy injection does not follow a PV or wind generation profile but is modelled as an infinite generator available at maximum capacity throughout all hours of the year. This allows to determine the technologically neutral maximum injectable energy from a grid perspective, maintaining operative security limits. The

determined DHC can then be used optimally by installations of different technologies (e.g. PV, wind, batteries), including hybridisation. RES uncertainty in the model refers to the output of preexisting generation units. Various yearly conditions of PV and wind resource availability are identified and employed combinatorically, i.e. every sample year of PV availability is evaluated against every sample year of wind availability due to often low correlations between PV and wind availability [30,31,32]. All preexisting generators are granted priority over the new generator under evaluation, i.e. HC cannot be enhanced by curtailing existing generation capacity (see merit order in 2).

Similar to SHC, DHC for normal operating conditions (DHC N) is contrasted with available DHC in the case of asset failures (DHC N-1). N-1 contingencies are modelled including network reconfigurations to ensure service availability in case of asset failure [29]. DHC N-1 is defined hour by hour as the minimum HC obtained from computing all N-1 contingencies.

2.3. Security-aware dynamic hosting capacity

Security-aware dynamic hosting capacity is defined as the network node's DHC accounting for N-1 contingencies and their probabilities. Instead of defining HC as the deterministic minimum value obtained throughout contingency operation, SDHC accounts for the failure probabilities of network assets. Similar to DHC, it represents an hourly curve for each node. SDHC assessment does not consider the mean time to failure of network assets. Instead, the optimal network configurations corresponding to N-1 contingency scenarios are simulated for each combination of yearly conditions. N-1 contingency HC is defined via DHC N-1 obtained for each network asset as described in 2.2.

Eq. (2) details the calculation of SDHC, where h represents the hour of the year,j represents the number of network assets accounted for SDHC calculation (i.e. all normally closed lines and transformers), and i indexes the network component under N-1 contingency.*FOR* represents the forced outage rate of the normally closed network assets.

$$SDHC_h = DHC_h^N \left[\prod_{j=1}^{N}(1-FOR_j)\right] + \sum_{i\in\Omega_{N-1}} DHC_{h,i}^{N-1} * FOR_i * \left[\prod_{\substack{j=1\\ j\neq i}}^{N}(1-FOR_j)\right] \quad (2)$$

3. Case study design

The modelling methodology is implemented in MATPOWER 7.1, employing the MATPOWER Interior Point Solver (MIPS) [33]. This section proceeds to present the distribution network employed for the case study (3.1) and details the input profiles for both load and existing RES generation (3.2), as well as the forced outage rate assumptions for N-1 modelling (3.3).

3.1. CIGRE benchmark network

Nodal HC is assessed with the CIGRE MV network with DER [34,35,36]. This radial benchmark distribution system operates at 20 kV (Fig. 2) and accounts for two downstream low voltage (LV) networks at nodes 1 and 12. This work defines security operating criteria according to the Spanish regulation. For this, thermal line limits are set to 70 % of a line's maximum capacity and maximum voltage deviations are limited to ± 7 % [37]. These limits align with UNE-EN 50,160 and are to be maintained during all static and dynamic hosting capacity scenarios. According to Spanish regulation, the specifications for HC assessment define that the SCR for each distribution network node must be greater than or equal to 6 [37]. These limits are applied to the CIGRE MV benchmark network.

Three sample nodes are selected for hosting capacity evaluation. The nodes are highlighted in yellow in Fig. 2. Node 3 is selected due to its proximity to the external grid, node 5 due to its location downstream in feeder 1, and node 14 due to its location in feeder 2.

N-1 contingencies are modelled under consideration of network reconfiguration using switches S1-S3 (Fig. 2). Failures of every normally

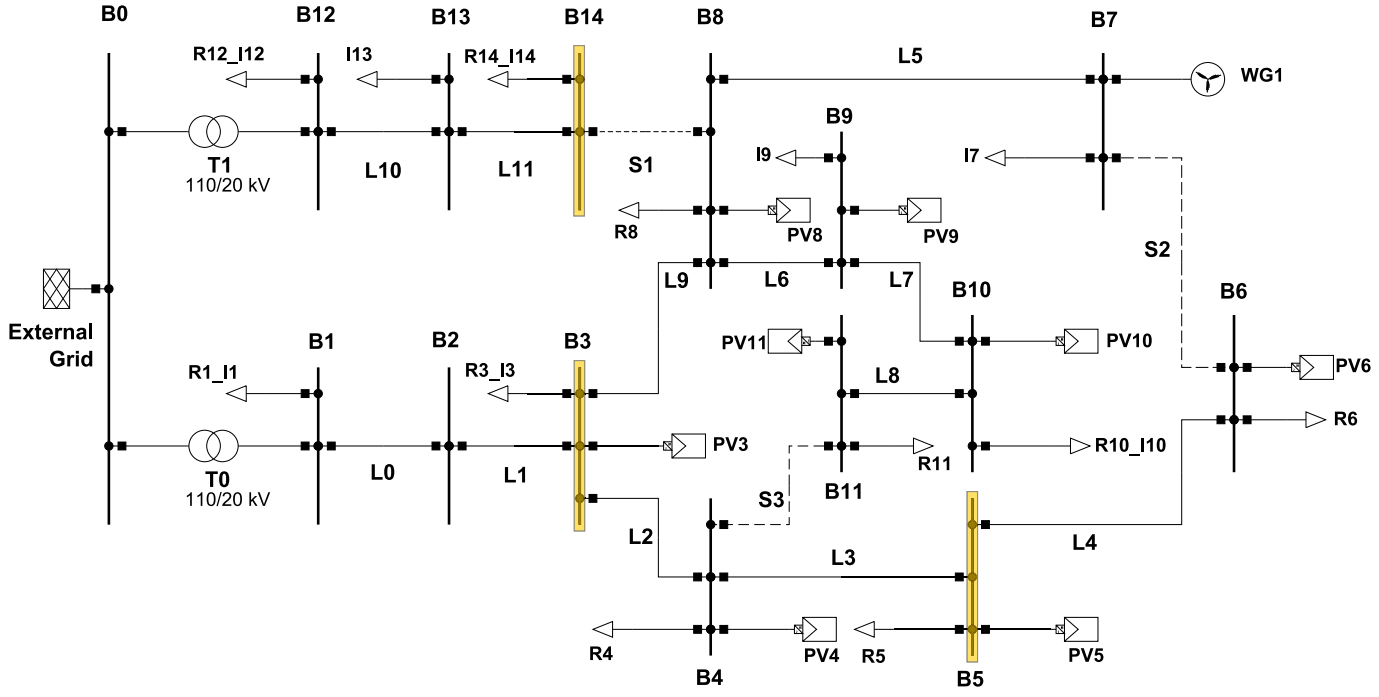

Fig. 2. Line diagram of the network.

closed line (L0 to *L*11) and both transformers are considered. Network reconfiguration is obtained via optimisation as in [29], and the results are annexed in Table 14.

3.2. Generation and load

3.2.1. Static reference scenario

The scenario for the calculation of SHC is determined according to Spanish regulation. Spanish DSOs are to evaluate the hosting capacity of their networks according to a reference scenario defined in regulation [28]. The scenario hypotheses are:

- **Minimum demand**: this demand is defined as 55 % of peak demand but can be substituted with minimum simultaneous system demand if sufficient data is available.
- **Maximum RES availability**: all generators connected to the grid and with permissions for connection granted are to be considered. At the node at which hosting capacity is evaluated, generators are considered at 100 % of their granted access capacity. At all other network nodes, generators are considered at 90 % of their granted access capacity.

3.2.2. Hourly load

Hourly load pu curves are extracted from the Spanish transparency platform ESIOS [38]. Residential load is assumed to follow the low voltage load curves, while commercial demand is assumed to follow the tariff category 6.1A, representing MV consumers [39]. Hourly curves are evaluated from 2015 to 2021 to determine the years with the greatest difference. A correlation analysis of the pre-crisis years shows no significant deviations in demand profiles throughout most of the years. Consequently, the pre-crisis year of 2019 is selected for load profiles. Furthermore, 2017 shows a seasonal variation from 2019 (Table 6) and is included in the analysis. Additionally, the load curves of 2021 are included in this analysis to account for the energy crisis years.

3.2.3. Hourly RES generation

The impact of RES generation uncertainty on HC is one of the key parameters to consider. Hence, several input profiles are selected to analyse the effect of RES stochasticity on the network's DHC. All curves represent RES availability in Almería, Spain and are derived from [40,41]. PV and wind curves evaluated for model input range from 2010 to 2022. In this work, RES variability is modelled via a combinatorial analysis of PV and wind generation profiles. Consequently, the 12 years of data on resource availability would lead to 144 RES years to model, leading to a total of 432 years due to the assessment of three load profile years. Due to the computational complexity of this issue, the amount of years to sample is reduced. Reducing the number of input curves is required for computational feasibility, as this analysis is carried out as a combinatorial analysis. The reduction of time series data is common in the literature [42]. The methodology for selecting sample years in this case study is not a novel contribution. It is chosen to select the sample years with a maximum variety. Thus, it allows to reduce computational effort while accounting for the variability of RES resource availability. In all cases, a very low correlation between solar and wind availability was observed (see Table 7 in the Annex).

As for PV, there is no significant variation throughout the years. The annexed Table 8 shows the correlations of the PV availabilities throughout the years 2010 to 2022. The lowest correlation is of 0.90. Hence, this metric is considered insufficient for selecting the study's sample years. Instead, years are selected based on the annual equivalent hours of the resource availability (Table 9). The years selected represent:

- High annual equivalent hours (2029 h in 2019)
- Medium annual equivalent hours (1972 h in 2016)
- Low annual equivalent hours (1911 h in 2010)

Table 1
Multi-criterion selection of wind resource sample years.

Year selected	Criteria
Y2014	Average annual equivalent hours; low CF at night, high CF during the afternoon; high CF in first months of the year
Y2015	Lowest annual equivalent hours
Y2016	Negative correlations with all years from 2018 onwards
Y2018	Highest monthly CF detected (March & April)
Y2021	Highest annual equivalent hours; high CF during night hours
Y2022	Low overall correlation with other years

For wind, the correlation analysis points out the randomness of resource availability (Table 10). Hence, a multi-criterion evaluation is carried out to reduce the sample years of wind resource availability. Criteria are annual equivalent hours (Table 11), average capacity factor (CF) per month of the year to express seasonality (Table 13), and average CF per hour of day (Table 13). The analysis allows to reduce the input profiles to six sample years, as explained in Table 1. As a result of the selection of sample years, DHC is derived from a combinatorial analysis of 3 load * 3 PV * 6 wind = 54 sample years instead of 432.

3.3. Network asset forced outage rates

For the computation of N-1 contingencies, the components' forced outage rates (FORs) are calculated. These FORs of the system components represent the probability of each N-1 contingency to happen. The probabilities are then applied to calculate the security-aware DHC.

Component failure rates are assumed to be of typical orders of magnitudes [43]. Table 2 shows an overview of the failure rate and the mean time to repair (MTTR) for overhead lines (OHL), cables and transformers.

These failure rates and the MTTR are applied to all normally closed network elements. Table 3 shows the resulting forced outage rates (FORs). The highest FOR is that of L1, with 0.057 %.

Table 2
Component failure rates [43].

Component	Failure rate λ *(per circuit mile and year)*	MTTR *(h)*
OHL	0.1	4
Cable	0.07	10
Transformer	0.04	40

Table 3
Forced outage rates of system components.

Element	Name	Type	Length *(km)*	FOR
L0	Line 1–2	Cable	2.82	0.036 %
L1	Line 2–3	Cable	4.42	0.057 %
L2	Line 3–4	Cable	0.61	0.008 %
L3	Line 4–5	Cable	0.56	0.007 %
L4	Line 5–6	Cable	1.54	0.020 %
L5	Line 7–8	Cable	1.67	0.021 %
L6	Line 8–9	Cable	0.32	0.004 %
L7	Line 9–10	Cable	0.77	0.010 %
L8	Line 10–11	Cable	0.33	0.004 %
L9	Line 3–8	Cable	1.3	0.017 %
*L*10	Line 12–13	OHL	4.89	0.036 %
*L*11	Line 13–14	OHL	2.99	0.022 %
T0	Transformer 0–1	25 MVA	–	0.018 %
T1	Transformer 0–12	25 MVA	–	0.018 %

4. Case study results

4.1. Static hosting capacity

As a first step of nodal HC assessment, SHC is determined according to the regulatory reference methodology. SHC is calculated for the reference scenario (section 2.1) under normal operating conditions (N), under N-1 contingencies, and according to the short-circuit ratio limitation. The minimum system demand of 13.7 MVA is detected on the 3rd of April of 2021 at 3 am, with commercial and residential loads at 30 % of their contracted capacity [34].

Fig. 3 shows an example of SHC determination under N-1 contingencies at node 5. The SHC for each contingency is compared to the reference scenario's SHC without contingency. The failure of lines connecting nodes 3 and 5 (L2 and L3) reduces the connectivity from node 5 with the rest of the network, reducing available HC. A failure in L9 has the same effect. Furthermore, failures affecting any line between L2 and L5 lead to the closure of S2. This is significant in the N-1 contingency scenario of L5, as it leads to a power flow from the wind farm towards the HC evaluation node, decreasing hosting capacity due to the priority of existing generation capacity. The smallest SHC at node 5 under N-1 contingency is 2.51 MW at a failure of L5.

Table 4 summarises the findings for the three nodes under evaluation. The N-1 criterion is the most limiting criterion at all of the nodes. This is hardly visible for node 3 but significantly reduces the SHC determined at nodes 5 and 14. As a result, the connection of new generation capacity to these network nodes is limited due to contingency considerations with minor FORs. At node 5, the minimum SHC is determined for the N-1 contingency at L5, as described above. At node 14, the N-1 contingency at *L*11 reduces the connectivity of node 14 and the residential demand feeder located at node 12, resulting in a SHC reduction of 2.02 MW from the 4.90 MW of SHC under normal operating conditions N.

Relaxing the SHC evaluation to normal operating conditions allows for + 30 % of injectable energy at node 5. At node 14, the additional injectable energy under SHC N compared to SHC N-1 is significant due to the magnitude of the reduction of SHC pointed out above. Compared to the restrictive SHC limited by contingency considerations at *L*11, SHC under normal operating conditions increases the injectable energy at node 14 by as much as 70 %. This finding underlines the value of introducing flexibility to be activated in low-probability events, i.e. relaxing the contingency consideration criterion for SHC assessment.

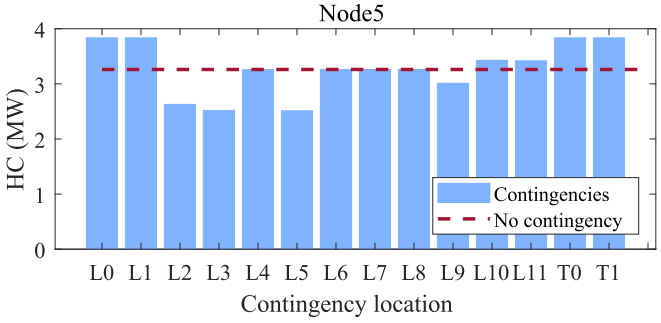

Fig. 3. SHC under N-1 contingencies for HC evaluation at node 5.

Table 4
SHC thresholds (MW) for each criterion of regulatory evaluation.

	Node 3	Node 5	Node 14
SHC N	3.25	3.26	4.90
SHC N-1	3.25	2.51	2.87
SCR	6.47	5.88	7.95
Limiting criterion	N-1 (L9)	N-1 (L5)	N-1 (*L*11)
Increase N vs N-1	0.13 %	+30 %	+70 %

4.2. Dynamic hosting capacity under normal operating conditions

After determining the SHC according to Spanish regulation, the network nodes' DHC is determined. The 18 years of hourly maximum injectable energy at the HC evaluation bus are evaluated as a load duration curve and compared to the SHC thresholds derived from regulation. For the sake of brevity, the analysis is carried out exemplary for one of the nodes under evaluation and compared to the other two nodes afterwards.

Fig. 4 presents the exemplary DHC load duration curves over the 54 sample years for node 5. DHC is compared to the different SHC thresholds according to the regulatory criteria. The figure shows the deviation between SHC N and the most restrictive SHC N-1 result mentioned previously (Table 4). Furthermore, the threshold derived from the short-circuit ratio is included in the figure. The filled blue area in Fig. 4 represents the maximum additional injectable energy in the case of DHC compared to the N-1 contingency SHC. The filled area represents an annual average of 67 % of injectable energy compared to the allowed injection under the N-1 restricted SHC.

Fig. 5 presents an analysis of DHC at node 5 throughout the hours of the day. This analysis is carried out to evaluate the dependence of HC and the input profiles. Hourly HC outputs of all 54 sample years are included in the boxplots. The figure points out that node 5 HC shows two peaks that coincide with the demand peaks of the Spanish electricity system, which does not vary throughout the sample years. The influence of the varying RES input profiles is not noticeable. The correlation between hourly hosting capacity and residential load is 0.99 at node 5. The correlations with RES profiles are insignificant: below 0.05 with wind and 0.35 with PV. The latter is influenced by the PV output peak coinciding with the central hours of the day when residential demand also peaks from 10:00 to 15:00.

Table 5 provides an overview of DHC under normal operating conditions N at the three nodes under analysis. DHC at all nodes is above the SHC threshold defined according to regulatory requirements, as indicated by the DHC N range in Table 5. DHC at node 14 shows a smaller range (4.64 MW to 5.2 MW) than the other nodes. Throughout the 54 sample years, DHC at node 14 is below SHC N for 83 h (0.018 %). At the other nodes, DHC is always above the regulatory reference scenario SHC N, pointing out the conservative assumptions of minimum load and

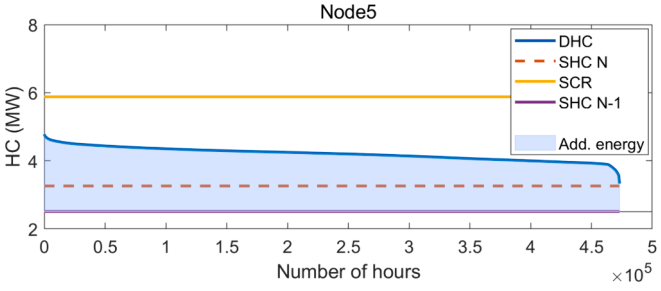

Fig. 4. Node 5 DHC load duration curve.

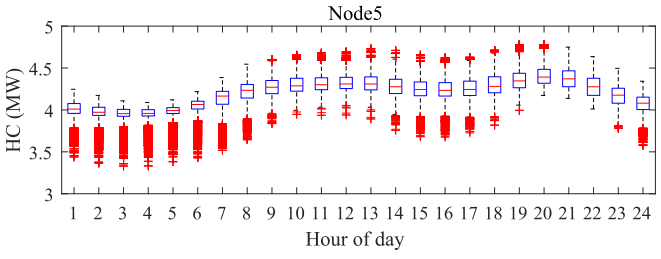

Fig. 5. Node 5 HC according to the hour of the day.

Table 5
Comparison of DHC results of nodes 3, 5 and 14 under normal operating conditions.

	Node 3	Node 5	Node 14
DHC range (N)	3.32 MW to 6.47 MW	3.33 to 4.78 MW	4.62 MW to 5.2 MW
Influent pu profiles	Residential load, wind	Residential load	Commercial load
Add. Energy/yr(DHC vs SHC N-1)	+62 %	+67 %	+76 %
Add. Energy/yr(DHC N-1 vs SHC N-1)	+34 %	+19 %	+27 %

maximum generation required for the reference scenario (2.1). DHC at node 5 ranges from 3.33 to 4.78 MW, while DHC at node 3 shows a significantly larger range (3.32 to the SCR cap of 6.47 MW). Node 3 is the only node where the SCR criterion limits DHC under normal operating conditions. The upstream location of node 3 close to the transformer station with a connected LV network increases the injectable energy. Node 14 is located in feeder 2, with no RES generation, resulting in HC depending on demand curves only, with a lower variability throughout the year. However, the increase from SHC to DHC is especially noticeable at node 14 due to the restrictive N-1 SHC result discussed in 4.1.

The evaluation of the impact of the input profiles on DHC results gives different results for the three nodes. At node 3, DHC depends on the residential load profile and the wind farm's energy output. The correlation with the wind profile is strongly negative (−0.7), indicating that HC at node 3 is reduced whenever the wind generator at node 7 injects energy into the network. This is explained by the location of the wind turbine in the network, which is relatively close to node 3. Power flow from the wind generator flows from node 7 to node 8, limiting the capacity of power flowing from node HC evaluation node 3 towards node 8. Furthermore, the correlations with load are positive, indicating that hours of high demand allow for a higher energy injection at network node 3. Correlations are higher with residential load (~0.6 to 0.7, depending on the load year) than commercial load (~0.4 to 0.5) due to residential load representing a higher share of network load. HC at node 14 again shows high correlations with load profiles. At this node, the commercial load profile has a higher impact on HC (correlation of > 0.9) than the residential load (~0.65 to 0.8, depending on the load year) due to the location of commercial loads at nodes 13 and 14. Injection at bus 14 allows for a decrease in imports from the upstream network to cover these loads. RES profiles do not impact DHC at node 14, as no generation capacity is located in feeder 2.

Furthermore, Table 5 includes the average annual injectable energy from the most restrictive SHC to DHC (represented as filled blue area in Fig. 4). The annual average is obtained by dividing the total additional injectable energy by 54 sample years. It is presented in MWh and as a percentual increase compared to the most restrictive SHC criterion. The lowest available additional injectable energy is of 62 % at node 3, representing a significant increase compared to the SHC. This additional injectable energy reaches as much as 76 % at node 14, where regulatory SHC is severely limited due to the N-1 contingency considerations.

4.3. Dynamic hosting capacity under N-1 contingencies

In the first step of the contingency analysis, DHC under N-1 contingencies is assessed individually for each N-1 contingency. The analysis evaluates the distribution functions of the 54 sample years of DHC for each contingency. Fig. 6 represents the cumulative distribution functions (CDFs) of DHC under N-1 contingencies for the three nodes under analysis. The CDF under normal operating conditions N is included. At node 3, N-1 failures in lines L0, L1 and L9 have a decreasing effect on the DHC, shifting the CDF towards the left. A failure in L0 or L1 results in the unavailability of node 3 to supply the demand in node 1, which represents loads of an entire LV system connected downstream of the MV grid. A contingency in L9 affects the downstream power flow from the node under HC consideration. Contingencies on feeder 2 (*L*10, *L*11, T1) have an increasing effect on DHC at node 3 due to the closure of S1 in these contingencies. This allows the supply of additional loads on feeder 2 via energy injection at node 3. The same is the case under the contingency of T0. The CDFs of both transformer contingencies show that energy injection is at the SCR limit during all hours. However, it should be noted that failures of the transformer stations lead to a significant amount of non-served energy despite increasing DHC at node 3. The remaining contingencies do not affect the DHC at node 3.

At node 5, no N-1 contingency leads to an increase in DHC. Contingencies in lines L2 to L5 lead to a decrease in HC. The maximum shift of the CDF to the left is observed at L3, followed by L5. Failures affecting any line between L2 and L5 lead to the closure of S2. This is significant in the N-1 contingency scenario of L5, as it leads to a power flow from the wind turbine towards node 5, decreasing hosting capacity due to the

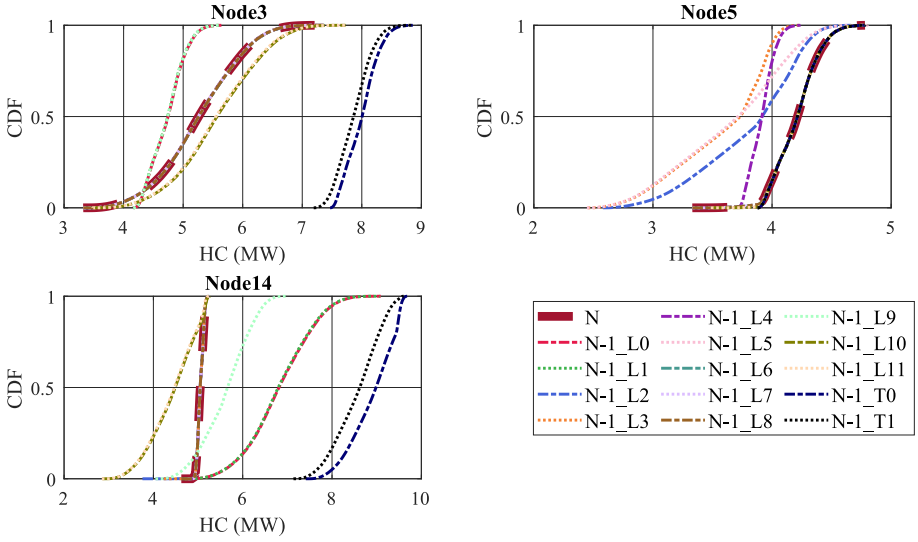

Fig. 6. Cumulative distribution functions of DHC under N-1 contingencies.

priority of existing generation capacity. The remaining contingencies do not affect the DHC at node 5.

At node 14, DHC increases at contingencies in L0 and L1 are significant. This is due to the closure of S1, allowing to supply the loads at feeder 1 via injecting energy at node 14. The same effect is observed in the case of a contingency at L9, although the increase is lower than in the case of L0 and L1. Similar to the observations at node 3, contingencies at the transformer stations increase the injectable energy at node 14 at the expense of significant amounts of non-served energy. The CDFs for both transformer contingencies are at the SCR during almost all hours. Contingencies located at feeder 2 ($L10$ and $L11$) reduce the connection of node 14 from the downstream LV network located at node 12, reducing hosting capacity under these contingencies. The remaining contingencies do not affect the DHC at node 14.

Table 5 includes information on the additional injectable energy for DHC N-1, derived from the least favourable N-1 HC for each hour of the year. The annual additional injectable energy is 34 % at node 3, 19 % at node 5, and 27 % at node 14. These percentages are based on the minimum N-1 contingency DHC result for each hour of the year, disrespecting the low probabilities of occurrence of these contingencies (Table 3).

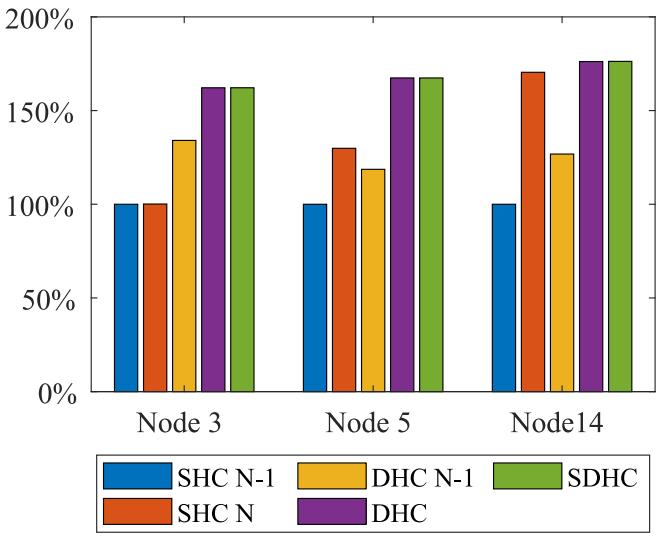

Fig. 8. Relative injectable energy – SHC, DHC and SDHC.

4.4. Security-aware dynamic hosting capacity

DHC results are evaluated under N-1 contingencies to obtain security-aware DHC. The SDHC is obtained by computing Eq. (2) with the FORs of each N-1 contingency (Table 3). Fig. 7 presents the annual SDHC for each node under evaluation. Furthermore, the N-1 range indicates the minimum and maximum hosting capacity under contingencies detected for each hour of the year. The dashed line represents the regulatory SHC (section 4.1). The 54 sample years are reduced to 8760 h by assigning each year equal weight.

The figure points out that, at nodes 3 and 14, maximum energy injections are limited by the short circuit ratio (SCR) threshold. SDHC at node 3 reaches the maximum SCR threshold several times throughout the year, while at node 14, only N-1 contingencies activate the SCR injection limit. All minimum SDHC values are above the threshold of SHC determined according to regulation.

The SDHC of node 3 shows the highest variability due to the negative correlation with the wind resource. Contrarily, the SDHC at node 14 shows the lowest variability throughout the year due to the high correlation with the commercial load profile and the lack of correlation with RES generation profiles. At node 5, the SDHC is at the upper bound of the N-1 range. N-1 contingencies only lower DHC at this node, as shown in Fig. 6.

Fig. 8 compares the annual injectable energy at each HC evaluation node. SHC under N-1 restrictions, SHC under normal operating conditions N, most limiting N-1 DHC, DHC under normal operating conditions, and SDHC are compared. The DHC N-1 data refers to the lowest line of the DHC range shown in Fig. 7. The energy injection in the SHC N-1 case is used as a baseline (100 %). The figure points out the potential of relaxing the N-1 contingency criteria for calculating SHC (see section 4.1). Furthermore, the figure points out the significant increase in injectable energy when comparing DHC to SHC (see section 4.2). Even the deterministic consideration of hourly worst-case N-1 DHC leads to an increase of annual injectable energy of at least 19 %. Due to the low values of FOR, SDHC does not show a significant variation from DHC. The variation is below 0.1 % at all three HC evaluation nodes. Consequently, compared to the N-1 restricted SHC, SDHC allows for an additional injectable energy of 62 %, 67 %, and 76 % at nodes 3, 5 and 14, respectively (i.e. the same values observed for DHC, Table 5). These values point out that, despite the N-1 range showing noticeable deviations from SDHC (Fig. 7), N-1 contingencies do not significantly affect DHC due to low FORs.

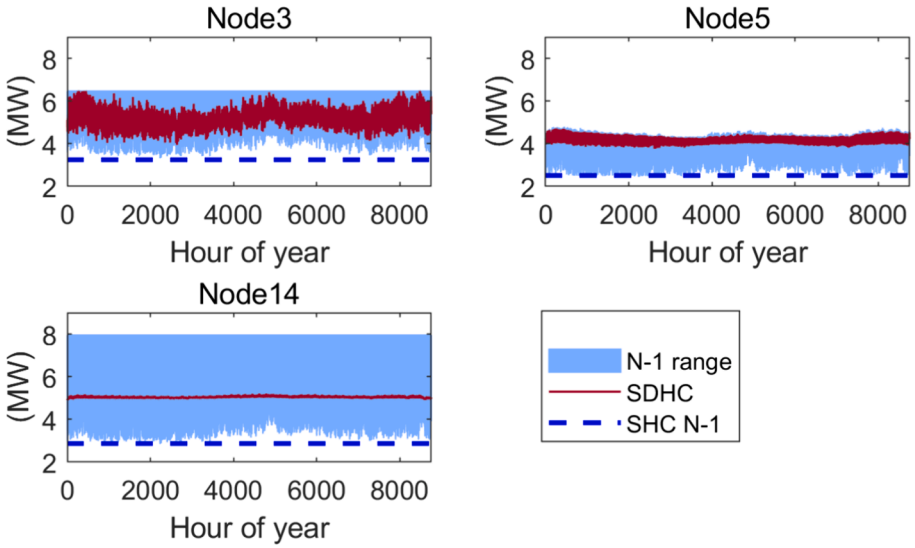

Fig. 7. Security-aware annual DHC.

5. Conclusions

This paper presents an analysis of a distribution network's security-aware dynamic hosting capacity under the uncertainty of RES generation profiles considering N-1 network contingencies. SDHC introduces a concept of dynamic hosting capacity accounting for N-1 asset contingencies and their probabilities. Dynamic hosting capacity allows to assess a network node's capacity for additional energy injection based on hourly values of demand and generation capacity instead of a static threshold derived via conservative operative assumptions. Hourly SDHC throughout the year is compared to the static hosting capacity threshold calculated according to Spanish regulatory requirements. The analysis is carried out for three different nodes of the CIGRE benchmark MV grid. Node 3 is selected due to its proximity to the external grid, node 5 due to its location downstream in feeder 1, and node 14 due to its location in feeder 2.

The evaluation of SHC shows that the regulatory requirement for considering N-1 network contingencies translates to a significant reduction of available HC despite forced outage rates of below 0.06 %. Consequently, DSOs are required to severely limit connections to their network based on considerations that are very unlikely to happen. Relaxing the contingency criteria for evaluating a network's hosting capacity could significantly increase the available HC of current electricity distribution grids. This study finds increases in annual injectable energy of up to 70 % when relaxing the N-1 contingency criterion, i.e. implementing low-probability event flexibility. This finding is based on the consideration of SHC according to conservative requirements without allowing for a more dynamic definition of hosting capacity.

The benefits of DHC are evaluated as hourly DHC over 54 sample years of different PV and wind generation profile years as well as load, obtained via a combinatorial analysis of three PV profiles and six wind profiles. Wind profiles are considered with a higher amount of sample years due to the randomness of the resource. A comparison of DHC with SHC under normal operating conditions shows that DHC falls below SHC thresholds only at node 14 and only during 0.018 % of the hours considered in the analysis. This observation points out the conservative assumptions of the regulatory reference scenario for evaluating SHC (close to maximum generation and minimum system demand).

The hourly computation of N-1 network asset failures' impact on DHC leads to the definition of the N-1 range. Even the worst-case DHC, that is the minimum hourly N-1 DHC, leads to an increase of annual injectable energy of at least 19 % when compared to N-1 SHC.

This paper defines the concept of security-aware dynamic hosting capacity as DHC accounting for the network's N-1 contingencies and their FORs. The evaluation of SDHC shows that some contingencies may even temporarily increase a network node's HC. However, due to low FORs, the variation of SDHC from average DHC under normal operating conditions is below 0.01 % of annual injectable energy. The analysis of N-1 contingencies and their probabilities highlights the conservative regulatory requirements for evaluating distribution network hosting capacity. A dynamic definition of hosting capacity instead of imposing restrictive N-1 SHC thresholds due to low contingency probabilities allows injecting significant additional energy into existing distribution networks without requiring reinforcement. This additional injectable energy under SDHC ranges from 62 % to 78 %.

Dynamic hosting capacity represents a valuable tool for an efficient electricity network integration of RES. It is especially relevant in the context of high connection times due to permitting associated with network reinforcement processes derived from conservative grid operating assumptions. This work contributes a methodology for the evaluation of DHC and the impact of N-1 contingencies on available DHC. The methodology is generalisable to other networks to evaluate the impact of asset FOR on DHC. For doing so, asset failure rate and MTTRmust be provided together with N-1 contingency configurations. Future research should evaluate the utility of the additional available injectable energy under SDHC for different RES technologies and their associated generation profile. Furthermore, allocating SDHC to a connection seeker requires transparency regarding curtailment probabilities and procedures. Different forms of flexible connection agreements should be investigated to foster the utilisation of the available hosting capacity of existing networks via SDHC.

CRediT authorship contribution statement

Leslie Herding: Writing – original draft, Visualization, Methodology, Investigation, Formal analysis. **Leonel Carvalho:** Writing – review & editing, Validation, Methodology, Conceptualization. **Rafael Cossent:** Writing – review & editing, Validation, Supervision, Conceptualization. **Michel Rivier:** Writing – review & editing, Validation, Supervision, Funding acquisition, Conceptualization.

Declaration of competing interest

The authors declare the following financial interests/personal relationships which may be considered as potential competing interests: Leslie Herding reports financial support was provided by Iberdrola Chair on Energy and Innovation. If there are other authors, they declare that they have no known competing financial interests or personal relationships that could have appeared to influence the work reported in this paper.

Data availability

All data used is publicly available in the referenced sources.

Acknowledgements

The authors would like to thank Orlando Valarezo for providing scenario input data, and Lukas Sigrist for the patience and support throughout the modelling process. The authors appreciate the funding for the mobility of professors and researchers in foreign research centres obtained from Universidad Pontificia Comillas.

This research has been carried out thanks to the Iberdrola Chair on Energy and Innovation and the funding of the RETOS COLABORACIÓN programme of the Spanish Ministry of Science and Innovation and the Spanish State Research Agency (project "Platform of innovative models to accelerate the energy decarbonisation of the economy (MODESC)", with reference number RTC2019- 007315-3).

Appendix. Load sample year selection

Table 6
Average residential load (pu) per month of the year.

	Y2015	Y2016	Y2017	Y2018	Y2019	Y2020	Y2021
January	0.69	0.66	0.67	0.64	0.69	0.67	0.65
February	0.68	0.67	0.61	0.67	0.63	0.58	0.55
March	0.58	0.63	0.55	0.60	0.56	0.54	0.53
Abril	0.50	0.57	0.49	0.53	0.54	0.47	0.48
May	0.50	0.53	0.49	0.49	0.50	0.45	0.46
June	0.54	0.57	0.57	0.53	0.53	0.50	0.48
July	0.66	0.64	0.59	0.59	0.63	0.62	0.54
August	0.57	0.62	0.58	0.60	0.59	0.59	0.53
September	0.52	0.60	0.52	0.55	0.54	0.52	0.49
October	0.51	0.54	0.50	0.51	0.52	0.51	0.46
November	0.56	0.62	0.57	0.58	0.60	0.55	0.54
December	0.60	0.68	0.65	0.61	0.63	0.64	0.57

PV and wind pu sample year selection.

Table 7
Annual correlations of PV and wind availability.

	Y2010	Y2011	Y2012	Y2013	Y2014	Y2015	Y2016	Y2017	Y2018	Y2019	Y2020	Y2021	Y2022
CORREL (PV,wind)	0.00	−0.03	−0.02	−0.02	−0.04	−0.01	0.01	−0.03	−0.02	−0.05	−0.02	−0.06	−0.03

Table 8
Correlations of PV availability between different years considered in the study.

	Y2010	Y2011	Y2012	Y2013	Y2014	Y2015	Y2016	Y2017	Y2018	Y2019	Y2020	Y2021	Y2022
Y2010		0.90	0.90	0.91	0.90	0.91	0.92	0.91	0.90	0.91	0.91	0.90	0.90
Y2011	0.90		0.92	0.92	0.92	0.92	0.93	0.92	0.92	0.92	0.92	0.91	0.91
Y2012	0.90	0.92		0.93	0.93	0.93	0.92	0.92	0.92	0.93	0.93	0.92	0.92
Y2013	0.91	0.92	0.93		0.93	0.93	0.93	0.93	0.92	0.93	0.92	0.91	0.93
Y2014	0.90	0.92	0.93	0.93		0.93	0.93	0.93	0.93	0.94	0.93	0.92	0.91
Y2015	0.91	0.92	0.93	0.93	0.93		0.93	0.93	0.92	0.94	0.93	0.92	0.93
Y2016	0.92	0.93	0.92	0.93	0.93	0.93		0.93	0.92	0.93	0.93	0.91	0.92
Y2017	0.91	0.92	0.92	0.93	0.93	0.93	0.93		0.92	0.93	0.93	0.91	0.92
Y2018	0.90	0.92	0.92	0.92	0.93	0.92	0.92	0.92		0.93	0.92	0.92	0.91
Y2019	0.91	0.92	0.93	0.93	0.94	0.94	0.93	0.93	0.93		0.93	0.93	0.92
Y2020	0.91	0.92	0.93	0.92	0.93	0.93	0.93	0.93	0.92	0.93		0.91	0.92
Y2021	0.90	0.91	0.92	0.91	0.92	0.92	0.91	0.91	0.92	0.93	0.91		0.91
Y2022	0.90	0.91	0.92	0.93	0.91	0.93	0.92	0.92	0.91	0.92	0.92	0.91	

Table 9
Equivalent hours of solar PV availability.

	Y2010	Y2011	Y2012	Y2013	Y2014	Y2015	Y2016	Y2017	Y2018	Y2019	Y2020	Y2021	Y2022
Eq. hours	1911	1949	2007	2007	2020	1989	1972	2017	1959	2029	1967	1951	1899

Table 10
Correlations of wind availability between different years considered in the study.

	Y2010	Y2011	Y2012	Y2013	Y2014	Y2015	Y2016	Y2017	Y2018	Y2019	Y2020	Y2021	Y2022
Y2010		-0.01	0.00	0.08	0.03	0.07	0.06	0.12	0.06	0.05	0.01	0.08	0.01
Y2011	-0.01		0.05	0.13	0.02	0.01	-0.01	0.10	0.16	0.10	0.02	-0.04	0.05
Y2012	0.00	0.05		0.00	0.10	0.06	0.06	0.07	0.07	0.04	0.06	-0.02	0.03
Y2013	0.08	0.13	0.00		0.12	0.03	0.01	0.08	0.06	0.07	0.04	0.06	0.08
Y2014	0.03	0.02	0.10	0.12		0.00	0.07	0.02	0.14	0.01	0.01	-0.01	0.05
Y2015	0.07	0.01	0.06	0.03	0.00		0.06	0.09	-0.02	0.00	0.07	0.06	0.00
Y2016	0.06	-0.01	0.06	0.01	0.07	0.06		0.04	-0.04	-0.04	-0.04	-0.04	-0.05
Y2017	0.12	0.10	0.07	0.08	0.02	0.09	0.04		0.07	-0.04	0.03	-0.01	0.00
Y2018	0.06	0.16	0.07	0.06	0.14	-0.02	-0.04	0.07		0.01	0.05	0.04	0.09
Y2019	0.05	0.10	0.04	0.07	0.01	0.00	-0.04	-0.04	0.01		0.08	0.05	0.01
Y2020	0.01	0.02	0.06	0.04	0.01	0.07	-0.04	0.03	0.05	0.08		0.03	0.02
Y2021	0.08	-0.04	-0.02	0.06	-0.01	0.06	-0.04	-0.01	0.04	0.05	0.03		0.05
Y2022	0.01	0.05	0.03	0.08	0.05	0.00	-0.05	0.00	0.09	0.01	0.02	0.05	

Table 11
Equivalent hours of wind availability.

	Y2010	Y2011	Y2012	Y2013	Y2014	Y2015	Y2016	Y2017	Y2018	Y2019	Y2020	Y2021	Y2022
Eq. hours	3742	3741	3401	3763	3546	3244	3634	3466	3654	3564	3421	3792	3644

Table 12
Average wind capacity factor per month of the year.

Month	Y2010	Y2011	Y2012	Y2013	Y2014	Y2015	Y2016	Y2017	Y2018	Y2019	Y2020	Y2021	Y2022
January	0.54	0.42	0.33	0.50	0.51	0.35	0.42	0.36	0.46	0.38	0.27	0.49	0.48
February	0.59	0.37	0.41	0.50	0.54	0.61	0.64	0.54	0.36	0.44	0.30	0.58	0.40
March	0.46	0.58	0.42	0.67	0.54	0.33	0.32	0.39	0.68	0.49	0.50	0.53	0.55
Abril	0.41	0.50	0.56	0.47	0.38	0.49	0.44	0.48	0.65	0.48	0.49	0.48	0.47
May	0.49	0.50	0.41	0.37	0.44	0.41	0.44	0.54	0.34	0.41	0.48	0.40	0.41
June	0.37	0.37	0.37	0.46	0.33	0.42	0.37	0.44	0.40	0.37	0.47	0.40	0.46
July	0.42	0.34	0.38	0.34	0.32	0.22	0.45	0.31	0.28	0.41	0.40	0.34	0.34
August	0.33	0.42	0.30	0.33	0.27	0.34	0.49	0.33	0.34	0.28	0.30	0.31	0.41
September	0.31	0.45	0.44	0.38	0.34	0.38	0.32	0.33	0.38	0.34	0.37	0.33	0.34
October	0.30	0.38	0.29	0.27	0.44	0.32	0.34	0.29	0.38	0.27	0.33	0.40	0.35
November	0.47	0.47	0.45	0.38	0.45	0.31	0.39	0.29	0.44	0.55	0.31	0.46	0.39
December	0.45	0.33	0.33	0.50	0.32	0.28	0.38	0.46	0.29	0.47	0.45	0.48	0.39

Table 13
Average wind capacity factor per hour of the day.

Hour	Y2010	Y2011	Y2012	Y2013	Y2014	Y2015	Y2016	Y2017	Y2018	Y2019	Y2020	Y2021	Y2022
1	0.40	0.41	0.37	0.41	0.39	0.36	0.39	0.38	0.41	0.41	0.38	0.41	0.41
2	0.40	0.41	0.37	0.41	0.39	0.35	0.40	0.39	0.41	0.41	0.38	0.41	0.41
3	0.40	0.41	0.37	0.42	0.38	0.35	0.40	0.39	0.41	0.40	0.39	0.42	0.41
4	0.40	0.41	0.37	0.42	0.38	0.36	0.40	0.39	0.40	0.40	0.38	0.42	0.41
5	0.41	0.42	0.37	0.43	0.37	0.36	0.40	0.39	0.40	0.40	0.38	0.42	0.41
6	0.42	0.42	0.37	0.43	0.36	0.37	0.40	0.39	0.39	0.39	0.38	0.42	0.40
7	0.42	0.42	0.36	0.42	0.36	0.37	0.40	0.39	0.38	0.38	0.38	0.42	0.39
8	0.42	0.42	0.36	0.42	0.35	0.36	0.40	0.39	0.37	0.38	0.37	0.42	0.39
9	0.42	0.42	0.36	0.42	0.35	0.36	0.40	0.38	0.37	0.37	0.36	0.41	0.39
10	0.42	0.42	0.36	0.42	0.35	0.35	0.40	0.38	0.38	0.37	0.37	0.41	0.39
11	0.42	0.42	0.37	0.42	0.37	0.36	0.40	0.39	0.39	0.38	0.37	0.42	0.40
12	0.43	0.42	0.38	0.42	0.39	0.36	0.41	0.39	0.41	0.39	0.38	0.42	0.41
13	0.44	0.43	0.39	0.43	0.41	0.37	0.42	0.40	0.43	0.40	0.39	0.43	0.42
14	0.44	0.44	0.40	0.44	0.43	0.38	0.43	0.40	0.45	0.42	0.40	0.44	0.43
15	0.45	0.44	0.41	0.44	0.45	0.39	0.44	0.41	0.46	0.44	0.41	0.46	0.44
16	0.46	0.45	0.42	0.45	0.46	0.40	0.45	0.42	0.46	0.45	0.42	0.46	0.44
17	0.47	0.45	0.43	0.46	0.47	0.41	0.46	0.43	0.47	0.45	0.43	0.47	0.45
18	0.47	0.46	0.44	0.47	0.47	0.41	0.46	0.43	0.47	0.46	0.44	0.48	0.45
19	0.46	0.46	0.43	0.46	0.46	0.40	0.45	0.42	0.45	0.44	0.43	0.47	0.44
20	0.44	0.44	0.42	0.45	0.45	0.39	0.43	0.40	0.44	0.43	0.41	0.46	0.43
21	0.43	0.42	0.40	0.43	0.43	0.37	0.42	0.39	0.42	0.41	0.39	0.44	0.41
22	0.42	0.42	0.39	0.42	0.42	0.37	0.40	0.38	0.42	0.40	0.38	0.43	0.41
23	0.41	0.41	0.39	0.41	0.41	0.36	0.40	0.38	0.41	0.40	0.38	0.42	0.41
24	0.40	0.41	0.38	0.41	0.40	0.36	0.39	0.38	0.41	0.41	0.38	0.42	0.41

Network reconfiguration.

Table 14
N-1 contingency reconfigurations (Line: failure element, column: state of each element in case of failure).

	L0	L1	L2	L3	L4	L5	L6	L7	L8	L9	L10	L11	T0	T1
L0	0	1	1	1	1	1	1	1	1	1	1	1	1	1
L1	1	0	1	1	1	1	1	1	1	1	1	1	1	1
L2	1	1	0	1	1	1	1	1	1	1	1	1	1	1
L3	1	1	1	0	1	1	1	1	1	1	1	1	1	1
L4	1	1	1	1	0	1	1	1	1	1	1	1	1	1
L5	1	1	1	1	1	0	1	1	1	1	1	1	1	1
L6	1	1	1	1	1	1	0	1	1	1	1	1	1	1
L7	1	1	1	1	1	1	1	0	1	1	1	1	1	1
L8	1	1	1	1	1	1	1	1	0	1	1	1	1	1
L9	1	1	1	1	1	1	1	1	1	0	1	1	1	1
L10	1	1	1	1	1	1	1	1	1	1	0	1	1	1
L11	1	1	1	1	1	1	1	1	1	1	1	0	1	1
L12	0	0	1	1	1	1	0	0	0	0	0	0	0	0
L13	0	0	0	0	0	0	1	1	1	0	0	0	0	0
L14	1	1	0	0	0	0	0	0	0	1	1	1	1	1
T0	1	1	1	1	1	1	1	1	1	1	1	1	0	1
T1	1	1	1	1	1	1	1	1	1	1	1	1	1	0

References

[1] European Commission, *Proposal for a COUNCIL REGULATION laying down a framework to accelerate the deployment of renewable energy*. 2022. Accessed: Sep. 13, 2023. [Online]. Available: https://eur-lex.europa.eu/legal-content/EN/TXT/?uri=CELEX%3A52022PC0591&qid=1669020920010.

[2] European Commission, COMMISSION RECOMMENDATION on speeding up permit-granting procedures for renewable energy projects and facilitating Power Purchase Agreements. 2022. Accessed: Sep. 13, 2023. [Online]. Available: https://eur-lex.europa.eu/legal-content/EN/TXT/?uri=PI_COM%3AC%282022%293219&qid=1653033569832.

[3] Deloitte, 'La planificación y la tramitación de las infraestructuras eléctricas para la Transición Energética', Deloitte Spain. Accessed: Oct. 21, 2022. [Online]. Available: https://www2.deloitte.com/es/es/pages/energy-and-resources/articles/planificacion-y-tramitacion-infraestructuras-electricas.html.

[4] Herding L, Cossent R, Rivier M, Chaves-Ávila JP, Gómez T. Assessment of electricity network investment for the integration of high RES shares: a Spanish-like case study. Sustainable Energy Grids Networks 2021;28:100561. https://doi.org/10.1016/j.segan.2021.100561.

[5] CEER, 'CEER Paper on Alternative Connection Agreements'. Accessed: Dec. 11, 2023. [Online]. Available: https://www.ceer.eu/documents/104400/-/-/e473b6de-03c9-61aa-2c6a-86f2e3aa8f08.

[6] Alturki M, Khodaei A, Paaso A, Bahramirad S. Optimization-based distribution grid hosting capacity calculations. Appl Energy Jun. 2018;219:350–60. https://doi.org/10.1016/j.apenergy.2017.10.127.

[7] M.H.J. Bollen N. Etherden Overload and overvoltage in low-voltage and medium-voltage networks due to renewable energy — Some illustrative case studies in 2011 2nd IEEE PES International Conference and Exhibition on Innovative Smart Grid Technologies 2011 1 8 10.1109/ISGTEurope.2011.6162645.

[8] European Commission, 'COM(2023) 757 final'. Accessed: Nov. 29, 2023. [Online]. Available: https://eur-lex.europa.eu/legal-content/EN/TXT/PDF/?uri=COM:2023:757:FIN.

[9] Scottish Power Ltd., 'Getting Connected-SP MANWEB HEAT MAPS', Getting Connected-SP MANWEB HEAT MAPS. [Online]. Available: https://www.spenergynetworks.co.uk/pages/sp_manweb_heat_maps.aspx.

[10] SP Energy Network, 'Getting Connected - SP DISTRIBUTION HEAT MAPS', SPEnergyNetworks. Accessed: May 11, 2021. [Online]. Available: <%=GetPageUrl%>.

[11] ENERGA-OPERATOR SA, 'Informacje o stanie przyłączeń w sieci'. Accessed: Dec. 09, 2020. [Online]. Available: https://energa-operator.pl/uslugi/przylaczenie-do-sieci/informacje-o-stanie-przylaczen.

[12] i-DE, 'Mapa de Capacidad'. Accessed: Feb. 13, 2023. [Online]. Available: https://www.i-de.es/conexion-red-electrica/produccion-energia/mapa-capacidad-acceso.

[13] E-REDES, 'Información sobre la Capacidad de la red E-REDES'. Accessed: Feb. 13, 2023. [Online]. Available: https://www.eredesdistribucion.es/instalaciones/informacion-sobre-la-capacidad-de-la-red.

[14] Gómez T, Cossent R, Chaves-Avila JP. Flexible network access, local flexibility market mechanisms and cost-reflective tariffs: three regulatory tools to foster decarbonized electricity networks. Oxford Energy Forum 2020;124:18–23. https://www.iit.comillas.edu/publicacion/mostrar_publicacion_working_paper.php.es?id=387.

[15] ENA, 'Rising to Britain's Net Zero Challenge'. Accessed: Dec. 14, 2023. [Online]. Available: https://www.energynetworks.org/assets/images/Publications/2023/231211-ena-rising-to-connections.pdf?1702549332.

[16] Ofgem, 'Access and Forward-Looking Charges Significant Code Review – Summer 2019 working paper', Access and Forward-Looking Charges Significant Code Review – Summer 2019 working paper. Accessed: Aug. 07, 2020. [Online]. Available: https://www.ofgem.gov.uk/publications-and-updates/access-and-forward-looking-charges-significant-code-review-summer-2019-working-paper.

[17] European Commission, 'Digitalisation of the European Energy System | Shaping Europe's digital future'. Accessed: Dec. 20, 2023. [Online]. Available: https://digital-strategy.ec.europa.eu/en/policies/digitalisation-energy.

[18] N. Etherden, M. Bollen, S. Ackeby, and O. Lennerhag, 'The transparent hosting-capacity approach – overview, applications and developments', presented at the International Conference and Exhibition on Electricity Distribution : 15/06/2015 - 18/06/2015, 2015. Accessed: May 10, 2021. [Online]. Available: http://urn.kb.se/resolve?urn=urn:nbn:se:ltu:diva-39121.

[19] Ismael SM, Abdel Aleem SHE, Abdelaziz AY, Zobaa AF. 'State-of-the-art of hosting capacity in modern power systems with distributed generation'. Renew Energy 2019;130:1002–20. https://doi.org/10.1016/j.renene.2018.07.008.

[20] Koirala A, Van Acker T, Dhulst R, Van Hertem D. 'Hosting capacity of photovoltaic systems in low voltage distribution systems: a benchmark of deterministic and stochastic approaches'. Renew Sustain Energy Rev 2022;155:111899. https://doi.org/10.1016/j.rser.2021.111899.

[21] Herding L, Cossent R, Rivier M. 'Enhancing RES grid connection via dynamic hosting capacity and hybridization', presented at the. IEEE Belgrade PowerTech Belgrade, Serbia: IEEE 2023;2023. https://doi.org/10.1109/PowerTech55446.2023.10202726.

[22] D. Fang et al. Deterministic and Probabilistic Assessment of Distribution Network Hosting Capacity for Wind-Based Renewable Generation in 2020 International Conference on Probabilistic Methods Applied to Power Systems (PMAPS), Aug 2020 1 6 10.1109/PMAPS47429.2020.9183525.

[23] Naciri S, Moufid I, El Markhi H. Dynamic hosting capacity of photovoltaic system analysis and enhancement using distributed SVC and STATCOM compensators: case study of a university building. Renewable Energy Focus 2023;45:123–32. https://doi.org/10.1016/j.ref.2023.03.002.

[24] Ding F, Mather B. On distributed PV hosting capacity estimation, sensitivity study, and improvement. IEEE Trans Sustainable Energy Jul. 2017;8(3):1010–20. https://doi.org/10.1109/TSTE.2016.2640239.

[25] Yuan J, Weng Y, Tan C-W. Determining maximum hosting capacity for PV systems in distribution grids. Int J Electr Power Energy Syst 2022;135:107342. https://doi.org/10.1016/j.ijepes.2021.107342.

[26] Hajeforosh S, Khatun A, Bollen M. Enhancing the hosting capacity of distribution transformers for using dynamic component rating. Int J Electr Power Energy Syst 2022;142:108130. https://doi.org/10.1016/j.ijepes.2022.108130.

[27] Jain AK, et al. Dynamic hosting capacity analysis for distributed photovoltaic resources—framework and case study. Appl Energy Dec. 2020;280:115633. https://doi.org/10.1016/j.apenergy.2020.115633.

[28] CNMC, 'Resolución de 20 de mayo de, de la Comisión Nacional de los Mercados y la Competencia, por la que se establecen las especificaciones de detalle para la determinación de la capacidad de acceso de generación a la red de transporte y a las redes de distribución' https://www.boe.es/eli/es/res/2021/05/20/ (4) 2021 Accessed: Sep. 13, 2021. [Online]. Available.

[29] Valarezo O, Chaves-Ávila JP, Gómez T. 'Multi-objective distribution network reconfiguration: application to a real large-scale distribution system'. Appl Energy 2024. vol. Under review.

[30] Widen J. Correlations between large-scale solar and wind power in a future scenario for sweden. IEEE Trans Sustainable Energy 2011;2(2):177–84. https://doi.org/10.1109/TSTE.2010.2101620.

[31] Couto A, Estanqueiro A. Assessment of wind and solar PV local complementarity for the hybridization of the wind power plants installed in Portugal. J Clean Prod 2021;319:128728. https://doi.org/10.1016/j.jclepro.2021.128728.

[32] Harrison-Atlas D, Murphy C, Schleifer A, Grue N. Temporal complementarity and value of wind-PV hybrid systems across the United States. Renew Energy 2022;201:111–23. https://doi.org/10.1016/j.renene.2022.10.060.

[33] R. D. Zimmermann and C. E. Murillo-Sánchez, 'MATPOWER User's Manual, Version 7.1'. Accessed: Jul. 24, 2023. [Online]. Available: https://matpower.org/docs/MATPOWER-manual.pdf.

[34] CIGRE, 'Benchmark Systems for Network Integration of Renewable and Distributed Energy Resources', e-cigre. Accessed: Oct. 26, 2023. [Online]. Available: https://e-cigre.org/publication/ELT_273_8-benchmark-systems-for-network-integration-of-renewable-and-distributed-energy-resources.

[35] K. Rudion, A. Orths, Z. A. Styczynski, and K. Strunz, 'Design of benchmark of medium voltage distribution network for investigation of DG integration', in *2006 IEEE Power Engineering Society General Meeting*, Jun. 2006, p. 6 pp.-. doi: 10.1109/PES.2006.1709447.

[36] University of Kassel and Fraunhofer IEE, 'CIGRE Networks — pandapower 2.4.0 documentation'. Accessed: Oct. 26, 2023. [Online]. Available: https://pandapower.readthedocs.io/en/v2.13.1/networks/cigre.html.

[37] CNMC 'Circular 1/2021' Accessed: Sep. 19 2021 [Online]. Available: https://www.boe.es/eli/es/cir/2021/01/20/1/con.

[38] REE, 'Bienvenido | ESIOS electricidad datos transparencia'. Accessed: Oct. 23, 2023. [Online]. Available: https://www.esios.ree.es/es.

[39] CNMC, *Resolución de 18 de marzo de 2021, de la Comisión Nacional de los Mercados y la Competencia, por la que se establecen los valores de los peajes de acceso a las redes de transporte y distribución de electricidad de aplicación a partir del 1 de junio de 2021*, vol. BOE-A-2021-4565. 2021, pp. 33575–33593. Accessed: Oct. 23, 2023. [Online]. Available: https://www.boe.es/eli/es/res/2021/03/18/(3).

[40] Pfenninger S, Staffell I. Long-term patterns of European PV output using 30 years of validated hourly reanalysis and satellite data. Energy 2016;114:1251–65. https://doi.org/10.1016/j.energy.2016.08.060.

[41] Staffell I, Pfenninger S. Using bias-corrected reanalysis to simulate current and future wind power output. Energy 2016;114:1224–39. https://doi.org/10.1016/j.energy.2016.08.068.

[42] Novo R, Marocco P, Giorgi G, Lanzini A, Santarelli M, Mattiazzo G. Planning the decarbonisation of energy systems: the importance of applying time series clustering to long-term models. Energy Conversion and Management: X 2022;15:100274. https://doi.org/10.1016/j.ecmx.2022.100274.

[43] R.E. Brown Electric power distribution reliability 2nd ed. 2017 CRC Press Boca Raton 10.1201/9780849375682.